



Article

# Photocatalytic Pretreatment of Commercial Lignin Using TiO<sub>2</sub>-ZnO Nanocomposite-Derived Advanced Oxidation Processes for Methane Production Synergy in Lab Scale Continuous Reactors

Yu-Ming Chu <sup>1,2</sup>, Hafiz Muhammad Asif Javed <sup>3,\*</sup>, Muhammad Awais <sup>4,\*</sup>, Muhammad Ijaz Khan <sup>5</sup> , Sana Shafqat <sup>3</sup>, Falak Sher Khan <sup>6</sup>, Muhammad Salman Mustafa <sup>7</sup>, Dawood Ahmed <sup>8</sup>, Sami Ullah Khan <sup>9</sup> and Rana Muhammad Arif Khalil <sup>10</sup> 

<sup>1</sup> Department of Mathematics, Huzhou University, Huzhou 313000, China; chuyming@zjhu.edu.cn

<sup>2</sup> Hunan Provincial Key Laboratory of Mathematical Modeling and Analysis in Engineering, Changsha 410114, China

<sup>3</sup> Department of Physics, University of Agriculture Faisalabad, Faisalabad 38000, Pakistan; sanashafqat.pml@gmail.com

<sup>4</sup> Department of Biochemistry, UIBB, Pir Meher Ali Shah Arid Agriculture University, Rawalpindi 46300, Pakistan

<sup>5</sup> Department of Mathematics and Statistics, Riphah International University I-14, Islamabad 44000, Pakistan; mikhan@math.qau.edu.pk

<sup>6</sup> Department of Biotechnology, University of Sialkot, Sialkot 51040, Pakistan; falakmahmand@gmail.com

<sup>7</sup> Department of Mechanical Engineering, Sahiwal Campus, COMSATS University Islamabad, Sahiwal 57000, Pakistan; msalmanmustafa@gmail.com

<sup>8</sup> Department of Medical Lab Technology, University of Haripur, Khyber Pakhtunkhwa 22620, Pakistan; biochem\_ahmed@yahoo.com

<sup>9</sup> Department of Mathematics, COMSATS University Islamabad, Sahiwal 57000, Pakistan; samikhan@cuisahiwal.edu.pk

<sup>10</sup> Department of Physics, Materials Simulation Research Laboratory, Bahauddin Zakariya University, Multan 66000, Pakistan; muhammadarif@bzu.edu.pk

\* Correspondence: m.asif.javed@uaf.edu.pk (H.M.A.J.); muhammad.awais@cuisahiwal.edu.pk (M.A.)



**Citation:** Chu, Y.-M.; Javed, H.M.A.; Awais, M.; Khan, M.I.; Shafqat, S.; Khan, F.S.; Mustafa, M.S.; Ahmed, D.; Khan, S.U.; Khalil, R.M.A. Photocatalytic Pretreatment of Commercial Lignin Using TiO<sub>2</sub>-ZnO Nanocomposite-Derived Advanced Oxidation Processes for Methane Production Synergy in Lab Scale Continuous Reactors. *Catalysts* **2021**, *11*, 54. <https://doi.org/10.3390/catal11010054>

Received: 7 December 2020

Accepted: 30 December 2020

Published: 2 January 2021

**Publisher's Note:** MDPI stays neutral with regard to jurisdictional claims in published maps and institutional affiliations.



**Copyright:** © 2021 by the authors. Licensee MDPI, Basel, Switzerland. This article is an open access article distributed under the terms and conditions of the Creative Commons Attribution (CC BY) license (<https://creativecommons.org/licenses/by/4.0/>).

**Abstract:** The photocatalytic pretreatment of lignocellulosic biomass to oxidize lignin and increase biomass stability has gained attention during the last few years. Conventional pretreatment methods are limited by the fact that they are expensive, non-renewable and contaminate the anaerobic digestate later on. The present study was focused to develop a metal-derived photocatalyst that can work with visible electromagnetic spectra light and oxidize commercial lignin liquor. During this project the advanced photocatalytic oxidation of lignin was achieved by using a quartz cube tungsten T3 Halogen 100 W lamp with a laboratory manufactured TiO<sub>2</sub>-ZnO nanoparticle (nanocomposite) in a self-designed apparatus. The products of lignin oxidation were confirmed to be vanillic acid (9.71 ± 0.23 mg/L), ferrulic acid (7.34 ± 0.16 mg/L), benzoic acid (6.12 ± 0.17 mg/L) and *p*-coumaric acid (3.80 ± 0.13 mg/L). These all products corresponded to 85% of the lignin oxidation products that were detectable, which is significantly more than any previously reported lignin pretreatment with even more intensity. Furthermore, all the pretreatment samples were supplemented in the form of feedstock diluent in uniformly operating continuously stirred tank reactors (CSTRs). The results of pretreatment revealed 85% lignin oxidation and later on these products did not hinder the CSTR performance at any stage. Moreover, the synergistic effects of pretreated lignin diluent were seen that resulted in 39% significant increase in the methane yield of the CSTR with constant operation. Finally, the visible light and nanoparticles alone could not pretreat lignin and when used as diluent, halted and reduced the methane yield by 37% during 4th HRT.

**Keywords:** lignin oxidation; AOP; PCO; TiO<sub>2</sub>-ZnO; CSTR

## 1. Introduction

Sustainable fuel production and the utilization of renewable energy such as bio-methane is a demand of the current era. The production of bio-methane and the reduction of carbon content in the environment is gaining great attention recently [1]. Therefore, due to the maximum availability of lignocellulosic biomass, it has an important role in 2nd generation biofuel production, specifically the production of methane by anaerobic digestion. During digestion the biodegradability is compromised due to very complex and inbound lignocellulosic structure and low methane yields [2], so pretreatment methods must be employed to access the available biomass after lignin removal. However, the lignin contents still interfere with anaerobic digestion unless they are reduced, modified or oxidized to certain derivatives. [3] Lignin conversion has always been a point of concern whenever researchers come to work with complex lignocellulosic biomasses. [4]. A number of approaches have previously been utilized to oxidize, break or convert lignin before further processing of biomass. These approaches mainly included chemical (acid-base), biological (enzymatic) and mechanical (grinding) pretreatment methods to help increase the bioavailability of usable biomass. These previously employed approaches have some strategic, economic and operational issues such as temperature, pressure, pH, clean up, lower outputs and contamination in the anaerobic digester [5].

Researchers are now looking for sustainable, low cost and reusable catalysts with some added advantages of high quality and reusability. Mainly, they are searching for such catalysts that are active in the visible spectrum and have low cost of operation. These features also ensure the reusability of the catalyst [6]. This approach has already been applied by Merlin et al. who used  $\text{TiO}_2$  as an visible light catalyst where they demonstrated the oxidization of lignin from lignocellulosic biomass and the effect of pretreatment on biogas production [7]. Free standing  $\text{TiO}_2$  nanowires were used by Hu et al. for the degradation of pharmaceuticals into various simpler organic compounds.  $\text{TiO}_2$  nanobelts have also been exploited for dye degradation into simpler aromatics while nitrogen-doped  $\text{Ta}_2\text{O}_5$  nanoflowers were analyzed for degradation of methylene blue using visible light [8–10]. The products of lignin oxidation are organic acids like vanillic acid, ferrulic acid, *p*-coumaric acid, benzoic acid etc. [11]. Many conventional pretreatment methods report the destruction of lignin and utilization of biomass in anaerobic digesters [12].

More recent among pretreatment methods for biomass are advanced oxidation processes (AOPs) that are carried out by using photoactive metal oxide (MO) mostly as nanoparticles. AOPs are often characterized as photocatalytic oxidation (PCO) when using a metal-derived nanoparticle with visible light activity properties. During AOPs photons are directly used to push out electron hole pairs and the redox reactions of involved nanoparticles and also different organic acids are produced via the breakdown of lignin [13]. This pretreatment mostly releases lignin, which is necessary to make the cellulose amenable to subsequent enzymatic attack during digestion and improve the biodegradability [14]. Many research efforts were performed and numerous studies are underway to prepare a less expensive, more efficient as well as stable photocatalyst but during investigations different barriers are frequently raised [15]. There are some metal oxides which absorb light in the visible range. Kobayakawa et al. first reported in 1989 metal oxides-based photocatalysts which had excellent lignin degradation power and the analyzed various oxidation products as well [16].

The utilization of metal oxides for treatment of wastewater for removal of organic pollutants has also achieved great attention using ultraviolet light as photocatalyst and gives considerable results [17]. The metal oxide excitation with light photons is higher than the bandwidth which facilitates the photo-oxidation approach. The more effective and efficient photocatalysts such as some metal oxides have numerous benefits including less toxicity, economy, stability, water insolubility and excellent excitation, also being very easily supported on specific surfaces such as glass or steel [18]. They usually work by absorbing electromagnetic waves and generating electron hole pairs and  $\text{OH}\bullet$  radicals through photo-oxidation and this activity is a key to optimize the removal of different

organic pollutants dyes, amines, etc. [19]. This manuscript discusses the manufacturing and usage of TiO<sub>2</sub>-ZnO for PCO of commercial lignin. The idea put forward in this study is to evaluate the effect of pretreated lignin on continuously stirred tank reactors (CSTRs) used for biogas production. This study was also examined whether the products of lignin oxidation halt the process at large or not. This project was also a pioneering approach in PCO of commercial lignin and its subsequent application for biogas production. Finally the idea was to introduce a cheap, renewable and sustainable catalyst for AOP.

## 2. Results and Discussion

### 2.1. XRD

The X-ray diffraction (XRF) technique was adopted for structural analysis of the samples. Bragg's law ( $n\lambda = 2d \sin \theta$ ) constructive interference rule was applied to analyze the differentially diffracting waves. XRD also used to detect the crystal structure as well texture orientation. An angle with range of  $2\theta$  was used for scanning in all directions which was attained by random orientation of synthesized powder-based samples and nanocomposites. The diffraction peaks also changed for d-spacing which was allowed to examine synthesized nanocrystals. The intensity as a function of diffraction angle (2 Theta) was measured at 20° to 70°. The results demonstrated that the samples were in line, indicating TiO<sub>2</sub>-ZnO phase. It can be confined that the TiO<sub>2</sub> particles in the samples are identified as anatase phase for the sharp diffraction peaks located at  $2\theta$  values of 25.3°, 48.1°, 56.5°, 62.8°, 66.4° and 67.9° and in all XRD patterns corresponding to (101), (200), (110), (103), (200) and (112) crystal planes, respectively (Figure 1).

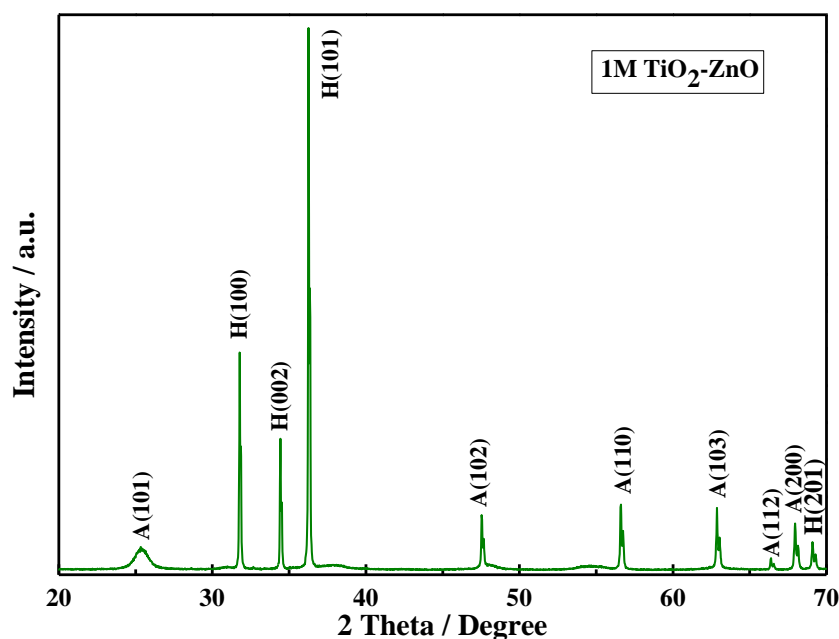
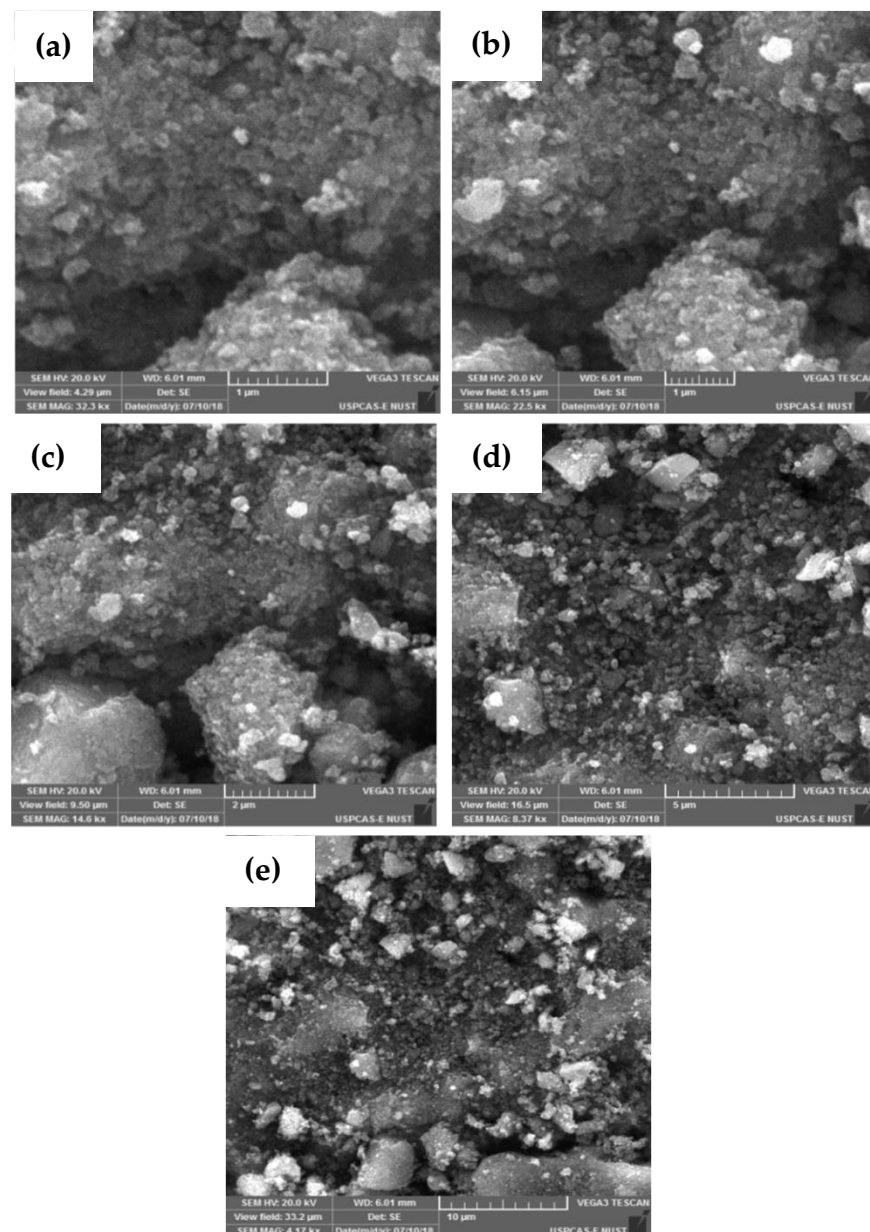


Figure 1. XRD result 1 M of TiO<sub>2</sub>-ZnO nanocomposite [A: Anatase, and H: Hexagonal].

Meanwhile it also has some ZnO diffraction peaks located at  $2\theta$  31.7°, 34.5°, 36.3° and 69.05°, which correspond to the (100), (002), (101) and (201) crystal planes, respectively [20]. There was significant difference in peaks of different molar ratios of TiO<sub>2</sub>-ZnO nanocomposite. These results confirm that as prepared TiO<sub>2</sub>-ZnO nanocomposite samples are the combination of anatase TiO<sub>2</sub> and hexagonal ZnO nanoparticles. It displayed that the samples were crystallized and a uniform lattice strain attained after annealing. It is stated that annealing to a higher temperature can increase the crystallinity TiO<sub>2</sub>-ZnO. Thus, ZnO and TiO<sub>2</sub>-ZnO were annealed at 500 °C [21]. Moreover, most diffraction peaks in the XRD patterns are sharp and symmetrical, which more signifies that the particles of TiO<sub>2</sub> and ZnO in the composite samples have high crystallinity [22].

## 2.2. Surface Morphology

The scanning electron microscopy (SEM) technique was used to study the morphological results under varying magnifications. In the SEM results the NO nanoparticles presented a spherical structure under  $49,000\times$  magnification (Figure 2). The surface morphology of  $\text{TiO}_2\text{-ZnO}$  nanocomposite calcined at  $500\text{ }^\circ\text{C}$  was analyzed using SEM analysis. The granular morphology of  $\text{TiO}_2\text{-ZnO}$  nanoparticles can be seen clearly in the following figures. SEM images for  $\text{TiO}_2\text{-ZnO}$  nanocomposite are displayed in Figure 2 and show that the size of the prepared particles was not more than  $500\text{ nm}$  [22].



**Figure 2.** SEM result M of  $\text{TiO}_2\text{-ZnO}$  nanocomposite (a)  $1\text{ }\mu\text{m}$  with  $4.29\text{ }\mu\text{m}$  field view (b)  $1\text{ }\mu\text{m}$  with  $6.15\text{ }\mu\text{m}$  field view (c) taken at  $2\text{ }\mu\text{m}$  (d) from  $5\text{ }\mu\text{m}$  (e) taken at  $10\text{ }\mu\text{m}$ .

Because of the high surface energy of the samples, they have the tendency to agglomerate and form the larger particles. Therefore, SEM results showed a strong agglomeration tendency with the average particle size of the aggregates. The result shows that Zn is uniformly disseminated into the  $\text{TiO}_2$  without disturbing the anatase as displayed in the XRD plots. The resulting SEM pictures displayed the presence of ZnO,  $\text{TiO}_2$  and  $\text{TiO}_2\text{-ZnO}$ .

### 2.3. EDX

Energy dispersive X-ray spectroscopy (EDX) was used to investigate the chemical stoichiometry of  $\text{TiO}_2\text{-ZnO}$  nanocomposite after heat treatment (Figure 3). The major and minor elemental composition was categorized by EDX, which showed the peaks corresponding to all the major and minor elements. Typical EDX results, for the different compositional ratios of  $\text{TiO}_2\text{-ZnO}$  nanocomposites at 500 °C annealing temperature are displayed in Table 1. The EDX results also show that Zn became a major component prior to executing the heat treatment procedure. The reason is that oxygen atoms are not fully arranged in ZnO which needs the heat treatment to get a better aligned structure. All the EDS results showing the presence of Zn, Ti and O elements. Signs of C impurities are detected in the EDX results.

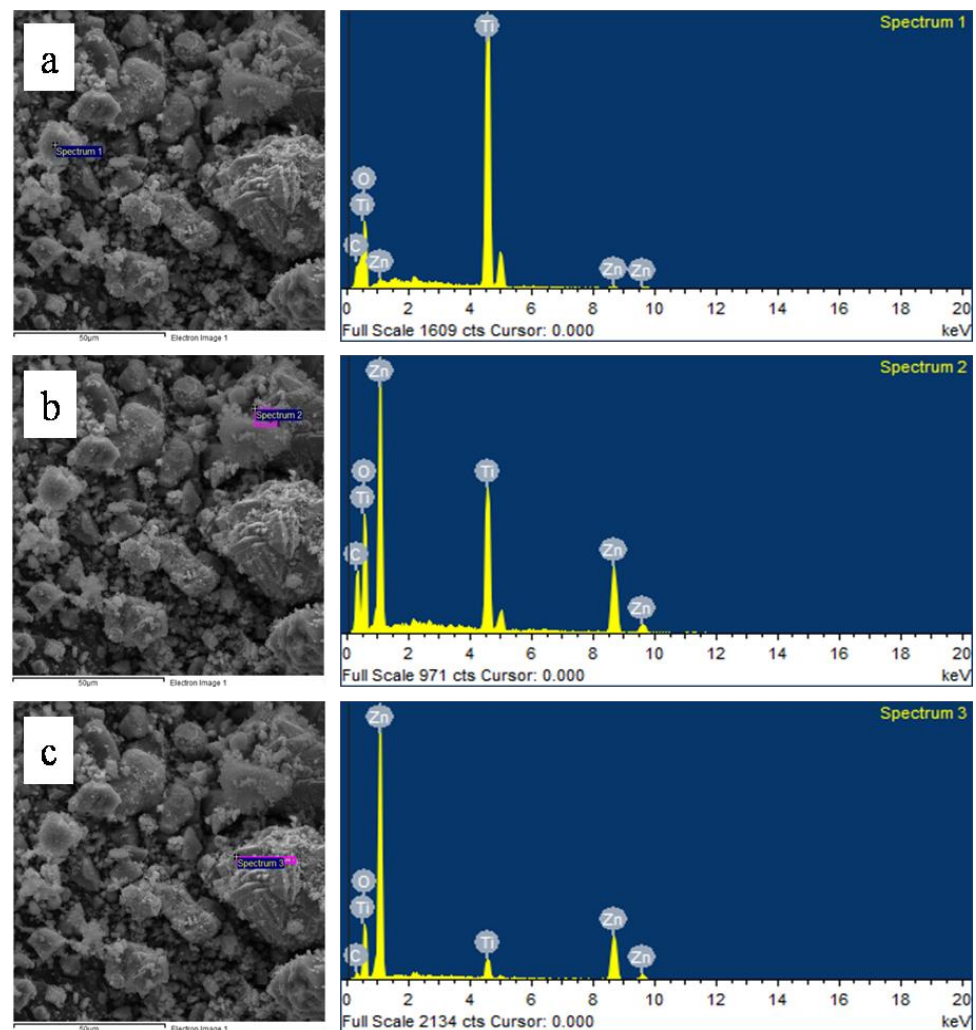


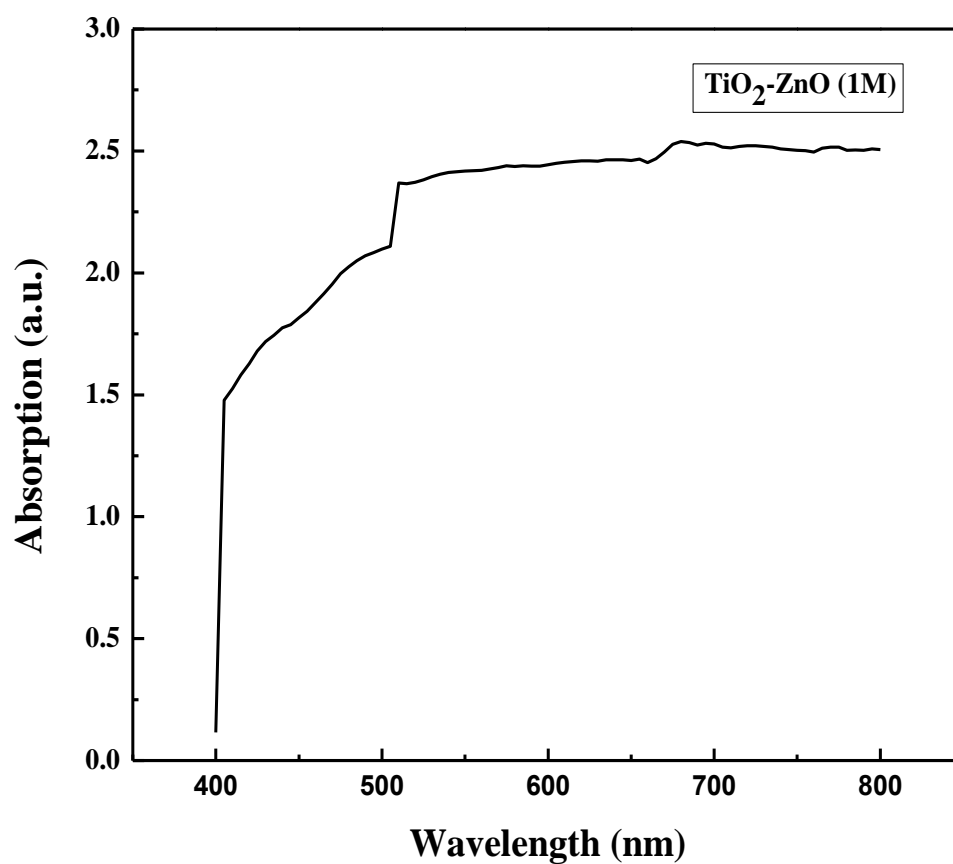
**Figure 3.** EDS results of  $\text{TiO}_2\text{-ZnO}$  nanocomposites: (a) Spectrum 1 (b) Spectrum 2 (c) Spectrum 3.

### 2.4. UV Spectroscopy

Optical properties were analyzed by ultraviolet-visible spectroscopy. The room temperature UV-visible absorbance spectra of a sample dispersed in absolute ethanol gives the following Figure 4, which shows the UV-visible absorption spectra of  $\text{TiO}_2\text{-ZnO}$  nanocomposite obtained at different charging voltages. After charging,  $\text{TiO}_2\text{-ZnO}$  nanocomposite shows significantly enhanced absorption intensity in the wavelength region from 400 nm to 800 nm.

**Table 1.** Compositional ratio of TiO<sub>2</sub>-ZnO nanocomposite at 500 °C annealing temperature.

	Element	Weight%	Atomic%
Spectrum 1	CK	14.04	23.06
	OK	50.74	62.57
	TiK	34.01	14.01
	ZnK	1.20	0.36
	Total	100.0	
Spectrum 1	CK	29.13	44.77
	OK	39.14	45.16
	TiK	10.81	4.16
	ZnK	20.93	5.91
	Total	100.0	
Spectrum 1	CK	13.15	25.63
	OK	38.63	56.54
	TiK	4.30	2.10
	ZnK	43.92	15.73
	Total	100.0	

**Figure 4.** UV result 1 M of TiO<sub>2</sub>-ZnO nanocomposite.

### 2.5. Analysis of Pretreatment Sets for Lignin Oxidation Products

Vanillic acid ( $9.71 \pm 0.23$  mg/L), ferrulic acid ( $7.34 \pm 0.16$  mg/L), benzoic acid ( $6.12 \pm 0.17$  mg/L) and *p*-coumaric acid ( $3.80 \pm 0.13$  mg/L) were determined as the main

lignin derivatives as a result of the POC process (Figure 5). These products correspond to 88% of the lignin oxidation products that were detectable, while previously reported amounts were significantly less compared to our 88% using the UV/TiO<sub>2</sub> system [11]. The VFA analysis and pH was categorized to study the variation caused by pretreatments which showed the pH was constant. There are some variations which may be due to the open system and volatile products. The PCO process was carried out using one double negative control having lignin and water only (Control 1), another with lignin in water with TiO<sub>2</sub>-ZnO but no exposure to light (Control 2) and finally lignin in water without TiO<sub>2</sub>-ZnO and exposed to light. All the results presented were taken from triplicate analyses and the deviations are also within the experimental range.

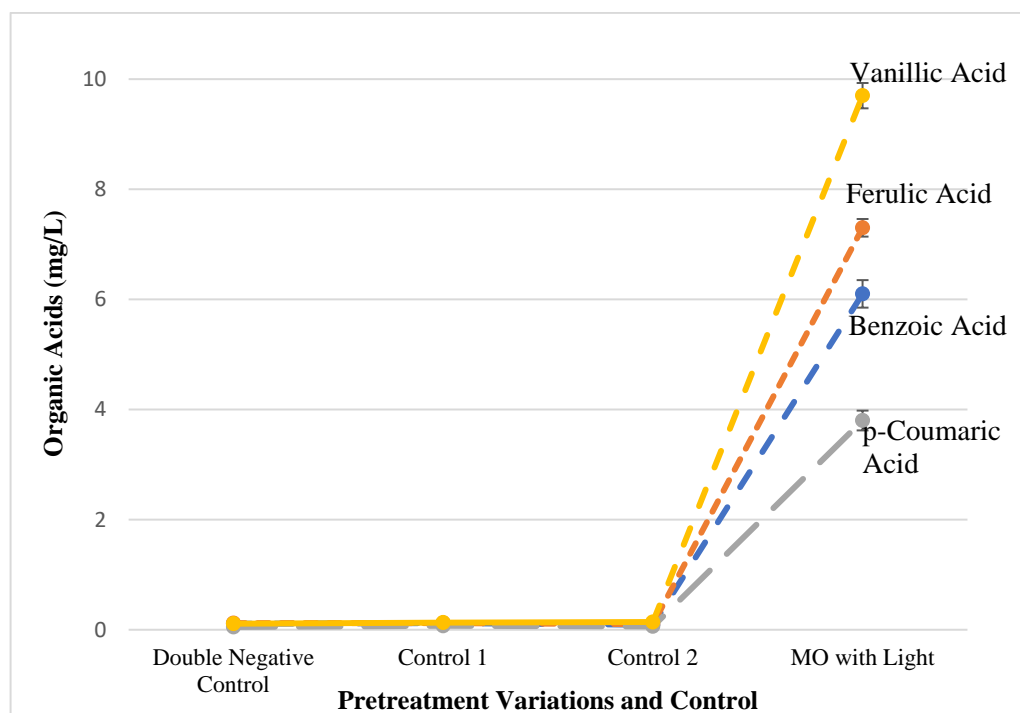


**Figure 5.** Analysis of lignin oxidation to organic acids during pretreatment in comparison with double negative and controls (1 and 2).

### 2.6. Methane Production Results from CSTRs

The CSTR was operated for 4 HRTs and first HRT was only meant to attain stability and at 16th day the substrate was diluted with pretreated lignin liquor. As a result of UHPLC the lignin oxidation products that were confirmed were now the part of reactor in 2nd and 3rd HRTs (days 16–45). During first HRT the average methane yield was recorded too be  $197.57 \pm 2.51$  mL CH<sub>4</sub>/gVS that reached to a maximum level of methane yield of  $284.65 \pm 3.83$  mLCH<sub>4</sub>/gVS and  $284.27 \pm 4.37$  for the 2nd and 3rd HRT. The noted increase in methane generation was noted to be 43%, which is significantly higher than the findings of [7] which were 25%. The CSTR steady state was very clearly explained by maintaining the VFAs and pH buildup which are presented in Table 2 having maintained the production of methane. This significant increase can be explained on the basis of the fact that lignin monomers such as vanillic acid, *p*-coumaric acid, ferulic acid, benzoic acid and syringic acid can be converted into methane under AD conditions [23]. Therefore, it can be established that when in 2nd and 3rd HRT CSTR was supplemented with pretreated lignin, its products were also converted to methane in addition to the normal feedstock. Hence, a positive synergism was also established that did not halt the methane production in any way. The sharp increase in methane yield and the lowering of yield to stabilization may be explained on the basis that microbial community trying to adapt to the change of diluent and the

products of lignin oxidation provided a synergistic boost in methane augmentation [24]. The methane yield presented in the CSTR results showed a significant enhancement of about 43% with a stable pH and VFA CSTR. The methane yield was maintained after a fast change in feedstock diluent at four days, as indicated by the results of the reactor in operation the steady methane yield in the second and third HRT. The contents of lignin oxidation did not hinder with CSTR at any stage during the 2nd and 3rd HRT that can be explained by the stable pH and VFAs. Furthermore, previously it was also reported that photocatalysis did not disturb ethanol production and that of other relevant products [25].

**Table 2.** Results from continuously stirred tank lab scale reactor for methane production in various HRTs, VFA and pH analysis throughout the operation of CSTRs.

	Days	Methane Average (NmLCH <sub>4</sub> /gVS)	pH Average Value	Average Total VFAs (mg/L)
HRT 1 (Day 1–15)	1–5	* 196.05 ± 1.53	7.89 ± 0.33	0.02 ± 0.00
	6–10	* 197.34 ± 2.03	7.91 ± 0.39	0.03 ± 0.00
	11–15	* 197.84 ± 2.51	7.94 ± 0.41	0.03 ± 0.00
HRT 2 (Day 16–30)	16–20	** 227.56 ± 3.41	7.92 ± 0.31	0.04 ± 0.00
	21–25	** 284.65 ± 3.83	7.99 ± 0.47	0.02 ± 0.00
	26–30	** 276.05 ± 4.42	8.01 ± 0.37	0.03 ± 0.00
HRT 3 (Day 31–45)	31–35	** 277.83 ± 3.89	8.01 ± 0.28	0.03 ± 0.00
	36–40	** 281.15 ± 4.01	7.98 ± 0.34	0.02 ± 0.00
	41–45	** 284.27 ± 4.37	7.91 ± 0.51	0.04 ± 0.00
HRT 4 (Day 46–60)	46–50	** 219.51 ± 3.81	7.89 ± 0.28	0.04 ± 0.00
	51–55	** 183.81 ± 2.91	7.92 ± 0.30	0.03 ± 0.00
	56–60	** 177.63 ± 3.01	7.97 ± 0.22	0.04 ± 0.00
HRT 5 (Day 61–75)	61–65	** 176.76 ± 3.74	7.88 ± 0.18	0.04 ± 0.00
	66–70	** 174.81 ± 3.62	7.94 ± 0.42	0.03 ± 0.00
	71–75	** 177.23 ± 4.61	7.95 ± 0.33	0.03 ± 0.00

\* Explains non-significant results during HRT 1. \*\* Explains significance of the results over HRT 1 average and individual values as well.

### 3. Methodology

#### 3.1. Synthesis of ZnO

ZnO nanoparticles were synthesized by a facile immersion method using zinc nitrate hexahydrate (Zn(NO<sub>3</sub>)<sub>2</sub>·6H<sub>2</sub>O), deionized water and a certain amount of ethanol which is needed to prevent the agglomeration of ZnO nanoparticles. More specifically, 1M solution contained 6 mL of distilled water, 4 mL of ethanol and 1 mole of zinc nitrate hexahydrate. Three different molar ratios of Zn(NO<sub>3</sub>)<sub>2</sub>·6H<sub>2</sub>O, viz. 0.25 M, 0.5 M and 1 M were prepared. These 0.25 M, 0.5 M and 1 M solutions were taken separately in separate beakers, after mixing all materials, solutions were stirred individually. Then, these solutions were annealed at 500 °C for 2 h to produce ZnO nanoparticles. After annealing we obtained the dried form of the ZnO, so to make its nanoform we had to grind it until nanoparticles are obtained [26].

#### 3.2. Synthesis of TiO<sub>2</sub>

TiO<sub>2</sub> nanopowder was synthesized by using a sol-gel method utilizing isopropyl alcohol (IPA) as solvent and titanium tetraisopropoxide (TTIP) as a metal precursor. Distilled water and HCl were used to maintain the pH. A molar ratio of 1:10 TTIP and IPA were mixed. Another solution of H<sub>2</sub>O and IPA with a molar ratio of 10:1 was prepared and TTIP plus IPA solution then stirred for an hour. This solution was then titrated into TTIP-IPA solution to produce colloidal uniform TiO<sub>2</sub> solution, this solution stirred for 2 h. The attained TiO<sub>2</sub> was analyzed in neutral pH by thermogravimetry. The TiO<sub>2</sub> solution is chemically highly unstable at neutral pH, so, it easily agglomerates when it converts into a gel form. This problem can be solved by adding acid to the solution, so HCl was added into



the TiO<sub>2</sub> sol to maintain its pH. Prepared TiO<sub>2</sub> sol is then dried in a microwave oven for 24 h to get nanoparticles, and the dried TiO<sub>2</sub> then ground till we get TiO<sub>2</sub> nanoparticles [27].

### 3.3. TiO<sub>2</sub>-ZnO Nanocomposite

For the synthesis of TiO<sub>2</sub>-ZnO nanocomposite, TiO<sub>2</sub> and ZnO nanopowders were mixed thoroughly and then calcined at 500 °C for 3 h to get TiO<sub>2</sub>-ZnO nanocomposite. The surface morphology, size, and structure of the nanocrystalline TiO<sub>2</sub>-ZnO nanoparticles were investigated in detail by scanning electron microscopy (SEM) (SEM-FEI Inspect™ S, Tokyo, Japan), X-ray diffractometry (XRD) (Ultima IV Multipurpose, Rigaku, Beijing, China) and ultraviolet visible (UV-vis) spectroscopy (T7S UV-vis Spectrophotometer, Thomas Scientific, Swedesboro, NJ, USA). In addition, energy dispersive X-ray analysis (EDX) is also employed to analyze the composite structure.

### 3.4. Photo-Catalytic Oxidation of Commercial Lignin

For the PCO of commercial lignin 30 mg/L of lignin was taken in pure water in a Pyrex beaker. For pretreatment a uniform sequence of steps was carried out for preparation of all sets as well observed under a UV lamp placed at a fixed 20 cm distance (Figure 6). In this work a quartz cube tungsten T3 halogen 100 W lamp was used, with 380–800 nm intensity [6]. The Li et al. approach was followed for pretreatment conditions and circumstances [28] and light exposure was performed for 4 h. The TiO<sub>2</sub>-ZnO weight concentration during pretreatment was taken as 4% TiO<sub>2</sub>-ZnO to the volume of lignin taken (*w/v*) [4]. The prepared pretreatment mixture was further divided into four parts. Three parts of the distributed pretreated mixture were used for methane production and one of the parts was separated to examine the organic acids obtained in the lignin oxidation process and further SEM and VFA analyses were also performed. The Hansen et al. protocol was used for calculation of the electrical energy per under observation solution [29]. PCO was carried out by using one double negative control having lignin and water only (Control 1), secondly, lignin in water with TiO<sub>2</sub>-ZnO but no exposure to light (Control 2) and thirdly, lignin in water without TiO<sub>2</sub>-ZnO and exposed to light. All the exposures were made for 4 h and the sets containing TiO<sub>2</sub>-ZnO had only 4% of this catalyst.

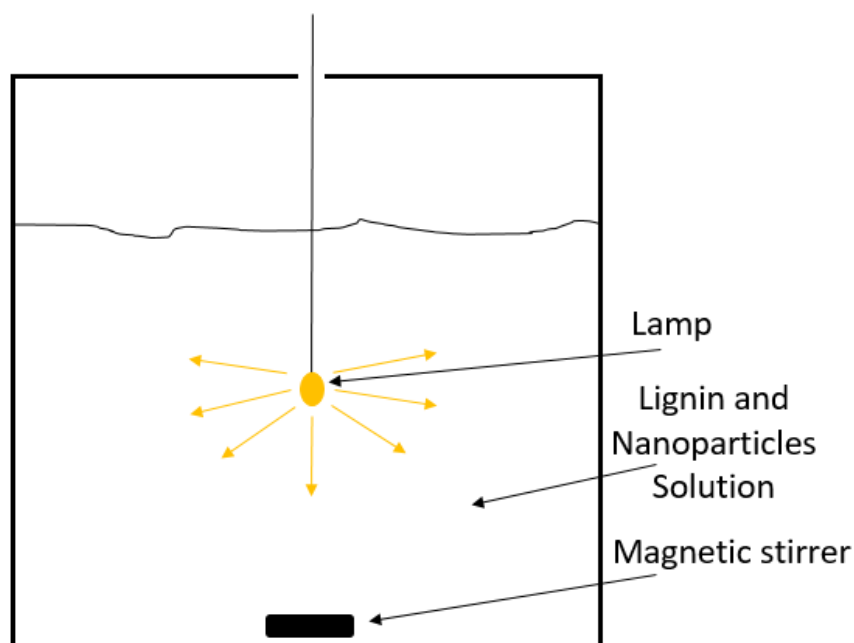
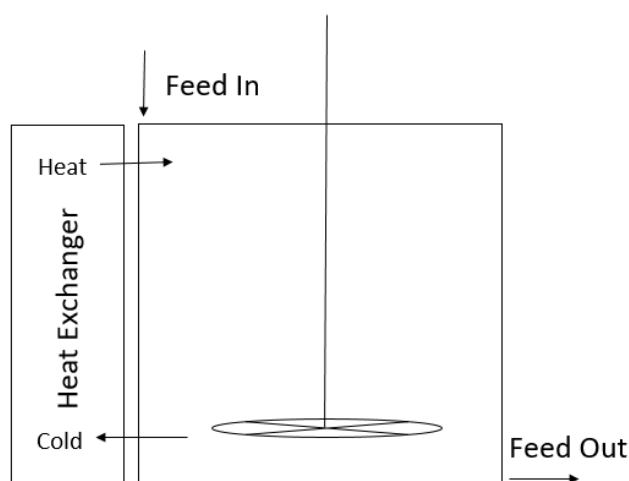


Figure 6. Schematic representation of the pretreatment apparatus.

### 3.5. PCO Product Supplementation CSTR Methane Production Units

The CSTR facility utilized in this study was operated with a 80:20 cattle manure to grasses ratio. The inoculum was taken from a local biogas plant (PMAS-Biogas Plant, Rawalpindi, Pakistan) at the university that was operated under constant conditions and inoculum degassing was performed prior to use in CSTRs. The inoculum and WS volatile solids were recorded  $92.8 \pm 0.4\%$ ,  $86.7 \pm 0.1\%$ ,  $2.8 \pm 0.1\%$  as well  $1.7 \pm 0.1\%$ , respectively, that are comparable to the findings of Kaparaju et al. [30]. Furthermore, the WS was examined based on TS in details for Klason lignin and structural carbohydrates resulting in cellulose  $42.0 \pm 0.7\%$ , hemicellulose  $30.8 \pm 0.5\%$  and Klason lignin  $26.7 \pm 2.7\%$ . Before CSTRs the inoculum was also examined for volatile fatty acids (VFAs) and  $0.2 \pm 0.0$  g/L acetate was recorded. There were some more fractions of VFAs also observed, such as butyrate, isobutyrate and isovalerate, which were present in very little amount and therefore considered as negligible. All the mentioned outcomes of VFAs were compared with the investigations of Tsapekos et al. and categorized [31].

A CSTR of 5.0 L volume from with a working volume (Figure 7) of 3 L was chosen for the continuous mode experiments. Further it was kept for 15 days of average hydraulic retention time (HRT) by maintaining a constant thermophilic temperature up to  $53 \pm 1$  °C. Through a modified feed pump the feed stock was modified via replacement of 100 mL of feedstock two times a day. The organic loading of this reactor was maintained at 0.8 gVS/L with the 20:80 ratio of grasses and cattle manure utilized for reactor operation. The liquid displacement method was applied for biogas volume measurement. VFAs composition and pH analysis of the reactors was measured twice a day and the average was presented. The total time of reactor operation was considered 60 days or up till four HRTs with each HRT being of 15 days in duration. During the first HRT the reactor with 80:20 cattle manure and grasses was operated to be normalized and stable. During the next two HRTs the water from the lignin oxidation experiments was taken and supplied as diluent of the substrates in CSTRs. From day 16–45 the water from pretreatment setup of 4% TiO<sub>2</sub>-ZnO/4 h was supplied as a diluent and in the last HRT (day 45–60) the mixed water from all controls (1, 2 and 3) of PCO was taken in ratio of 1:1:1, respectively.



**Figure 7.** Schematic of the CSTR Reactor.

### 3.6. Analytical Methods

Standard protocols were used to determine total and Kjeldahl nitrogen (TKN), total solids (VS), volatile solids (TS) and ammonium nitrogen (NH<sub>4</sub>-N) [32]. Strong acid hydrolysis was used for lignin and structural carbohydrate determination [33]. Furthermore, the pH of the prepared samples was also measured by using a PHM 92 LAB pH-meter (MeterLab<sup>TM</sup>, Copenhagen, Denmark). The Kougiass et al. [34] described protocol was used for VFA analysis of the pretreatments and inoculum by using a 4-methylvaleric acid

standard. More specifically the VFA analysis was performed by gas chromatography (GC) analysis via an auto-sampler (Kugelman and McCarty 1965, Shimadzu GC-8A, Tokyo, Japan). A GC Clarus 500 system was used (Perkin-Elmer Waltham, MA, USA) with a split/split-less injector and methane contents from biomethane potential (BMP) reactors were investigated using a flame ionization detector (FID). A GC chromatograph (GC-8A, Shimadzu, Tokyo, Japan) was utilized for methane contents determination with a flame ionization detector (FID). The observation and calculations were implemented in triplicate. An Agilent 1260/1290 Infinity UHPLC (Gentech, New York, NY, USA) system was also used to analyze the lignin oxidation products using the embedded Multiple Wavelength Detector (MWD-3000 RS Gentech, New York, United states). For contents separation a flow rate of 1 mL/min of the recommended 70/30 (by volume) acetic and acetonitrile acid mixture was used. A thermionic tungsten gun equipped (SEM-FEI Inspect S) scanning electron microscope was utilized for analysis of the nanoparticles. A large detector equipped with higher vacuum mode was also used to investigate the samples' morphology in SEM.

### 3.7. Statistical Analysis

The production of methane between BMP sets was also calculated and presented graphically via using Microsoft Excel (version 2007). Also all collected data was observed in terms of standard deviations and descriptive statistics. The most important way to investigate the analysis of variance (ANOVA) was used to justify the means of different groups in triplicate investigation with the described criterion of  $p < 0.05$ .

## 4. Conclusions

In this research work, the biomass pretreatment for 4 h with 4% nanocomposites showed an excellent yield of methane with 39% more average methane production compared with HRT 1. This up to 39% more The methane with CSTRs was observed because of the synergism between the lignin oxidation products and anaerobic digestion process. Moreover, the reactor contents were stable in all HRTs during the change of feed and operationally during the HRT days. Only the light from a lamp operating in the visible range was needed to pretreat the biomass excellently to perform PCO of lignin by AOP which produced mainly vanillic acid, ferrulic acid, *p*-coumaric acid and benzoic acid as lignin derivatives. It was also observed that the process of PCO is a very beneficial approach for pretreatment of biomass and lignin oxidation under the described circumstances. Due to the non-toxic nature, low cost and reusability of metal oxide nanoparticles the need to develop a sustainable and more reliable catalyst can be fulfilled. Furthermore, a pretreatment operated under visible spectrum light was also investigated instead of UV spectrum light. HRT 4 clearly indicated that alone light or nanocomposites could not pretreat the lignin and CSTR production depleted to even less than HRT 1 due to the presence of more undigested lignin.

**Author Contributions:** Data curation, S.U.K.; Formal analysis, F.S.K. and R.M.A.K.; Investigation, S.S.; Software, M.S.M.; Supervision, M.A.; Validation, D.A.; Writing—original draft, H.M.A.J. and M.A.; Writing—review & editing, Y.-M.C., M.A. and M.I.K. All authors have read and agreed to the published version of the manuscript.

**Funding:** This research received no external funding.

**Data Availability Statement:** Authors agree to the terms and conditions mentioned at <https://www.mdpi.com/ethics>.

**Acknowledgments:** The research was supported by National Natural Science Foundation of China (Grant Numbers 1191142, 11871202, 61673169, 11701176, 11626101 and 11601485).

**Conflicts of Interest:** The authors declare that they have no known competing financial interests or personal relationships that could have appeared to influence the work reported in this paper.

## References

1. Mittal, S.; Dai, H.; Fujimori, S.; Masui, T. Bridging greenhouse gas emissions and renewable energy deployment target: Comparative assessment of China and India. *Appl. Energy* **2016**, *166*, 301–313. [[CrossRef](#)]
2. Neshat, S.A.; Mohammadi, M.; Darzi, G.N.; Lahijani, P. Anaerobic co-digestion of animal manures and lignocellulosic residues as a potent approach for sustainable biogas production. *Renew. Sustain. Energy Rev.* **2017**, *79*, 308–322. [[CrossRef](#)]
3. Kabir, F.; Gulfraz, M.; Raja, G.K.; Inam-Ul-Haq, M.; Awais, M.; Mustafa, M.S.; Khan, S.U.; Tlili, I.; Shadloo, M.S. Screening of native hyper-lipid producing microalgae strains for biomass and lipid production. *Renew. Energy* **2020**, *160*, 1295–1307. [[CrossRef](#)]
4. Zhu, L.; Awais, M.; Javed, H.M.A.; Mustafa, M.S.; Tlili, I.; Khan, S.U.; Shadloo, M. Photo-catalytic pretreatment of biomass for anaerobic digestion using visible light and Nickle oxide (NiOx) nanoparticles prepared by sol gel method. *Renew. Energy* **2020**, *154*, 128–135. [[CrossRef](#)]
5. Awais, M.; Musmar, S.A.; Kabir, F.; Batool, I.; Rasheed, M.A.; Jamil, F.; Khan, S.U.; Tlili, I. Biodiesel Production from Melia azedarach and Ricinus communis Oil by Transesterification Process. *Catalysts* **2020**, *10*, 427. [[CrossRef](#)]
6. Awais, M.; Mustafa, M.S.; Rasheed, M.A.; Jamil, F.; Naqvi, S.M.Z.A. Metal Oxides and Ultraviolet Light-Based Photocatalytic Pretreatment of Biomass for Biogas Production and Lignin Oxidation. *BioResources* **2020**, *15*, 1747–1762.
7. Alvarado-Morales, M.; Tsapekos, P.; Awais, M.; Gulfraz, M.; Angelidaki, I. TiO<sub>2</sub>/UV based photocatalytic pretreatment of wheat straw for biogas production. *Anaerobe* **2017**, *46*, 155–161. [[CrossRef](#)]
8. Alvarado-Morales, M.; Tsapekos, P.; Awais, M.; Gulfraz, M.; Angelidaki, I. Hydrothermal growth of free standing TiO<sub>2</sub> nanowire membranes for photocatalytic degradation of pharmaceuticals. *J. Hazard. Mater.* **2011**, *189*, 278–285.
9. Hu, A.; Liang, R.; Zhang, X.; Kurdi, S.; Luong, D.; Huang, H.; Servos, M.R. Enhanced photocatalytic degradation of dyes by TiO<sub>2</sub> nanobelts with hierarchical structures. *J. Photochem. Photobiol. A Chem.* **2013**, *256*, 7–15. [[CrossRef](#)]
10. Shi, X.; Ma, D.; Ma, Y.; Hu, A. N-doping Ta<sub>2</sub>O<sub>5</sub> nanoflowers with strong adsorption and visible light photocatalytic activity for efficient removal of methylene blue. *J. Photochem. Photobiol. A Chem.* **2017**, *332*, 487–496. [[CrossRef](#)]
11. Ksibi, M.; Amor, S.B.; Cherif, S.; Elaloui, E.; Houas, A.; Elaloui, M. Photodegradation of lignin from black liquor using a UV/TiO<sub>2</sub> system. *J. Photochem. Photobiol. A Chem.* **2003**, *154*, 211–218. [[CrossRef](#)]
12. Awais, M.; Alvarado-Morales, M.; Tsapekos, P.; Gulfraz, M.; Angelidaki, I. Methane production and kinetic modeling for co-digestion of manure with lignocellulosic residues. *Energy Fuels* **2016**, *30*, 10516–10523. [[CrossRef](#)]
13. Mottweiler, J.; Puche, M.; Räuber, C.; Schmidt, T.; Concepción, P.; Corma, A.; Bolm, C. Copper-and Vanadium-Catalyzed Oxidative Cleavage of Lignin using Dioxygen. *ChemSusChem* **2015**, *8*, 2106–2113. [[CrossRef](#)] [[PubMed](#)]
14. Mosier, N.; Wyman, C.; Dale, B.; Elander, R.; Lee, Y.; Holtzapple, M.; Ladisch, M.R. Features of promising technologies for pretreatment of lignocellulosic biomass. *Bioresour. Technol.* **2005**, *96*, 673–686. [[CrossRef](#)]
15. Rawalekar, S.; Mokari, T. Rational design of hybrid nanostructures for advanced photocatalysis. *Adv. Energy Mater.* **2013**, *3*, 12–27. [[CrossRef](#)]
16. Kobayakawa, K.; Sato, Y.; Nakamura, S.; Fujishima, A. Photodecomposition of kraft lignin catalyzed by titanium dioxide. *Bull. Chem. Soc. Jpn.* **1989**, *62*, 3433–3436. [[CrossRef](#)]
17. Al-Dawery, S.K. Photo-Catalyst Degradation of Tartrazine Compound in Wastewater Using TiO<sub>2</sub> and UV Light. *J. Eng. Sci. Technol.* **2013**, *8*, 683–691.
18. Kumar, S.G.; Devi, L.G. Review on modified TiO<sub>2</sub> photocatalysis under UV/visible light: Selected results and related mechanisms on interfacial charge carrier transfer dynamics. *J. Phys. Chem. A* **2011**, *115*, 13211–13241. [[CrossRef](#)]
19. Lacombe, S.; Keller, N. *Photocatalysis: Fundamentals and Applications*; Wiley-Interscience: New York, NY, USA, 1989.
20. Abd Samad, N.A.; Lai, C.W.; Lau, K.S.; Abd Hamid, S.B. Efficient Solar-Induced Photoelectrochemical Response Using Coupling Semiconductor TiO<sub>2</sub>-ZnO Nanorod Film. *J. Mater.* **2016**, *9*, 937. [[CrossRef](#)]
21. Nanakkal, A.R.; Alexander, L.K. Photocatalytic Activity of Graphene/ZnO Nanocomposite Fabricated by Two-Step Electrochemical Route. *J. Chem. Sci.* **2017**, *129*, 95–102. [[CrossRef](#)]
22. Wang, L.; Fu, X.; Han, Y.; Chang, E.; Wu, H.; Wang, H.; Li, K.; Qi, X. Preparation, Characterization, and Photocatalytic Activity of TiO<sub>2</sub>/ZnO Nanocomposites. *J. Nanomater.* **2013**, *2013*, 1687–4116. [[CrossRef](#)]
23. Castellán, A.; Vanucci, C.; Bouas-Laurent, H. Photochemical Degradation of Lignin through  $\alpha$  C—O Bond Cleavage of Non Phenolic Benzyl Aryl Ether Units. A Study of the Photochemistry of a (2', 4', 6'-Trimethyl-Phenoxy)-3, 4 Dimethoxy Toluene. *Holzforsch.-Int. J. Biol. Chem. Phys. Technol. Wood* **1987**, *41*, 231–238. [[CrossRef](#)]
24. Healy, J.B.; Young, L.Y. Anaerobic Biodegradation of Eleven Aromatic Compounds to Methane. *Appl. Environ. Microbiol.* **1979**, *38*, 84–89. [[CrossRef](#)] [[PubMed](#)]
25. Yasuda, M.; Miura, A.; Yuki, R.; Nakamura, Y.; Shiragami, T.; Ishii, Y.; Yokoi, H. The effect of TiO<sub>2</sub>-photocatalytic pretreatment on the biological production of ethanol from lignocelluloses. *J. Photochem. Photobiol. A Chem.* **2011**, *220*, 195–199. [[CrossRef](#)]
26. Javed, H.M.A.; Que, W.; Yin, X.; Xing, Y.; Shao, J.; Kong, L.B. ZnO/TiO<sub>2</sub> nanohexagon arrays heterojunction photoanode for enhancing power conversion efficiency in dye-sensitized solar cells. *J. Alloys Compd.* **2016**, *685*, 610–618. [[CrossRef](#)]
27. Lim, C.S. Synthesis and characterization of TiO<sub>2</sub>-ZnO nanocomposite by a two-step chemical method. *J. Ceram. Process. Res.* **2010**, *11*, 631–635.
28. Li, H.; Lei, Z.; Liu, C.; Zhang, Z.; Lu, B. Photocatalytic degradation of lignin on synthesized Ag–AgCl/ZnO nanorods under solar light and preliminary trials for methane fermentation. *Bioresour. Technol.* **2015**, *175*, 494–501. [[CrossRef](#)]

29. Hansen, K.M.S.; Zorzea, R.; Piketty, A.; Vega, S.R.; Andersen, H.R. Photolytic removal of DBPs by medium pressure UV in swimming pool water. *Sci. Total Environ.* **2013**, *443*, 850–856. [[CrossRef](#)]
30. Kaparaju, P.L.-N.; Serrano, M.; Thomsen, A.B.; Kongjan, P.; Angelidaki, I. Bioethanol, biohydrogen and biogas production from wheat straw in a biorefinery concept. *Bioresour. Technol.* **2009**, *100*, 2562–2568. [[CrossRef](#)]
31. Tsapekos, P.; Kougias, P.G.; Angelidaki, I. Anaerobic mono-and co-digestion of mechanically pretreated meadow grass for biogas production. *Energy Fuels* **2015**, *29*, 4005–4010. [[CrossRef](#)]
32. American Public Health Association (APHA). *Standard Methods for the Examination of Water and Wastewater*; APHA: Washington, DC, USA, 2005.
33. Sluiter, A.; Hames, B.; Ruiz, R.; Scarlata, C.; Sluiter, J.; Templeton, D.; Crocker, D.L.A.P. Determination of structural carbohydrates and lignin in biomass. *Lab. Anal. Proced.* **2008**, *1617*, 1–16.
34. Kougias, P.; Boe, K.; Tsapekos, P.; Angelidaki, I. Foam suppression in overloaded manure-based biogas reactors using antifoaming agents. *Bioresour. Technol.* **2014**, *153*, 198–205. [[CrossRef](#)] [[PubMed](#)]